

## **CHAPTER THREE**

---

CHARACTERIZATION AND INVESTIGATION OF THE VERSATILITY AND ROBUSTNESS  
OF THE OPTIMIZED PORE-REGULATED POLYMER MATRIX FORMULATION UTILIZING  
PHENYTOIN SODIUM AND CARBAMAZEPINE AS MODEL DRUGS

### 3.1. INTRODUCTION

In Chapter two, the fabrication, mechanistic evaluation and optimization of the P-RPM formulation demonstrating controlled drug release and *ex vivo* buccal mucosal permeation characteristics was achieved. In addition, the effects of different levels of formulation variables on the overall performance of the P-RPM formulation were investigated. This new, specialized drug delivery system has to date not been explored by any other research group or applied in drug delivery employing the described approach. Consequently, it is imperative to characterize it and assess its robustness and versatility as regards its possible applicability for the delivery of a wide range of drugs employed for therapeutic purposes. In addition to this, the dissolution characteristics of the optimized P-RPM formulation separately loaded with either PS or CBZ will be compared with the commonly utilized commercially available oral tablet products in order to further evaluate its effectiveness.

Research has shown that drug release from polymer-based matrix systems is mainly controlled by polymer erosion and dissolution, swelling, drug dissolution and diffusion through the polymeric matrix at the molecular level. These phenomena depend upon the interaction between the dissolution media which is usually aqueous-based and the entire polymeric matrix as well as the model drug (Jamzad *et al.*, 2005). The dissolution media has to penetrate the polymer matrix leading to polymer swelling, relaxation or dissolution followed by drug solubilization and diffusion out of the matrix. These processes can be influenced by several formulation variables which include but are not limited to the drug concentration, drug solubility, permeability, polymer particle size, drug to polymer ratio, polymer solubility and viscosity, polymer molecular mass and the addition of different types and levels of excipients or release modulators (Velasco, 1999; Dürig and Fassihi, 2000; Pillay and Fassihi, 2000a and 2000b; Williams III *et al.*, 2002; Jamzad *et al.*, 2005). Among these parameters, drug solubility and permeability play a very important role in modulating the rate and degree of drug release by impacting the diffusion and dissolution of the drug molecules as well as permeation through mucosal sites (Li *et al.*, 2008).

The current Chapter focuses on characterizing the optimized P-RPM formulation as well as investigating its versatility and robustness by examining the effects of the differences in the physicochemical properties of phenytoin sodium (Solubility: 100mg/mL at 25°C and log P = 2.14) (Darwish *et al.*, 1996; Kasim *et al.*, 2004) and carbamazepine (Solubility: 0.01mg/mL at

25°C and  $\log P = 2.93$ ) (Kasim *et al.*, 2004; Koester *et al.*, 2004; Dong *et al.*, 2007). These objectives were accomplished by measuring and comparing characteristic physicochemical and physicomechanical parameters which are relevant to the performance of the optimized P-RPM formulation. The physicochemical parameters evaluated included drug release, drug loading capacity, *ex vivo* bioadhesivity, rheological viscosity and deformation, surface morphology, *ex vivo* drug permeation and porosimetric quantities while the physicomechanical parameters measured were matrix resilience, energy of matrix deformation and matrix rigidity. Besides, the release characteristics of phenytoin sodium and carbamazepine from the optimized P-RPM formulation were compared with the commonly utilized commercially available products.

## **3.2. EXPERIMENTAL SECTION**

### **3.2.1. Materials**

The optimized P-RPM formulation developed in Chapter two was employed in this experimental phase (Sections 2.2.13 and 2.3.10). Carbamazepine was purchased from Sigma Chemical Company (St. Louis, USA). The commercially available leading market products namely Epanutin<sup>®</sup> (phenytoin sodium) and Tegreto<sup>®</sup>CR (carbamazepine) were procured from Pfizer Limited, Johannesburg, South Africa and Novartis Pharmaceuticals Corporation, Isando, South Africa respectively. All other materials used are the same as in Chapter two (Section 2.2.1).

### **3.2.2. Fabrication of the optimized P-RPM formulation**

The optimized P-RPM formulation was prepared in accordance with the procedural specifications described in Section 2.2.2 of Chapter two. The quantities of the formulation variables employed in the construction of this optimized formulation are the same as those specified in Section 2.3.10 (Table 2.11) of Chapter two. CBZ was incorporated into the ethanol-based co-particulate dispersion after which the homogenous blend was formed. On the other hand, PS was included in the water-based dispersion as already mentioned in Chapter two (Section 2.2.2). 50mg of either of the model drugs, PS and CBZ, were separately loaded unto respective matrices for the physicochemical and physicomechanical analyses.

### **3.2.3. Evaluation of the physicochemical properties of the optimized P-RPM formulations**

As mentioned earlier, the physicochemical parameters studied were drug release, drug loading capacity, *ex vivo* drug permeation, *ex vivo* bioadhesivity, quantitative evaluation of matrix porosity, surface morphology and rheological measurements. These physicochemical

assessments were performed on the PS and CBZ loaded optimized P-RPM formulations according to the procedures explained in Sections 2.2.4, 2.2.5, 2.2.6, 2.2.7, 2.2.8.1, 2.2.9 and 2.2.10 of Chapter two respectively. All determinations were done in triplicate.

#### **3.2.4. Measurement of physicochemical parameters**

The physicochemical characteristics of the optimized P-RPMs were investigated using textural profile analysis. The specific parameters determined included the matrix resilience ( $M_R$ ), energy of matrix distortion ( $E_D$ ) and matrix firmness ( $M_F$ ) using a calibrated TA.XTplus Texture Analyzer (Stable Micro Systems, Surrey, England). These physicochemical parameters are defined in Chapter two (Section 2.3.9) of this thesis. In order to assess these parameters, the textural settings and methodology described in Chapter two (Section 2.2.11) were employed.

#### **3.2.5. Preparation of calibration curves for PS and CBZ in simulated saliva and plasma**

The calibration curves for PS dissolved in simulated saliva (pH 6.8) and plasma (pH 7.4) are already presented in Chapter two (Figure 2.3 (a) and (b); Section 2.2.12). For CBZ, the stock solution was prepared by separately dissolving 10mg of drug in 100mL of simulated saliva and plasma respectively. From the stock solutions, a series of dilute standard solutions of the following concentrations: 0.004, 0.008, 0.012 and 0.017 mg/mL were prepared by separately using simulated saliva and plasma. The absorbance of each standard solution was determined at the maximum wavelength of 285nm. Afterward, linear calibration curves for CBZ in simulated saliva and plasma (*simulated saliva:  $y=57.781x$ ;  $R^2=0.994$  and simulated plasma:  $y=59.299x$ ;  $R^2=0.981$* ) were generated (Figures 3.1 (a) and (b)).

#### **3.2.6. Treatment of *in vitro* drug release**

In order to provide thorough, concise and meaningful comparisons and explanations to the generated drug release profiles, both model-dependent and model independent analyses were employed.

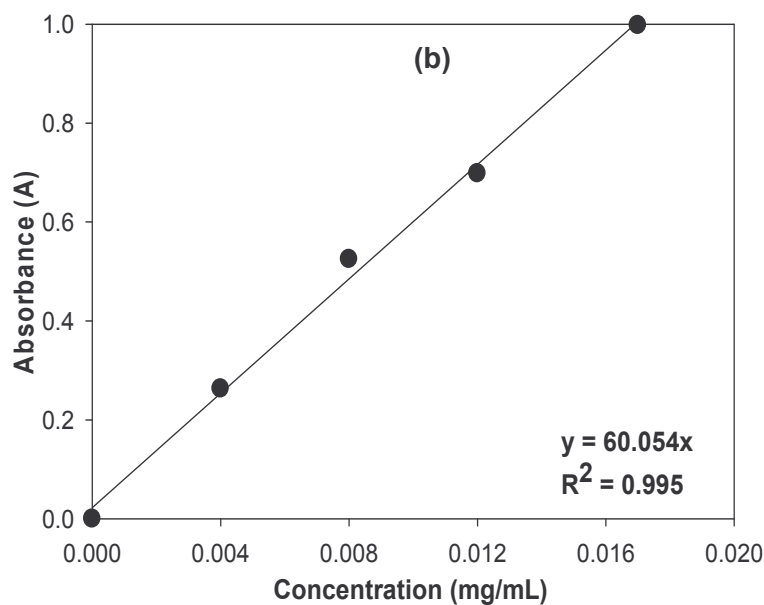
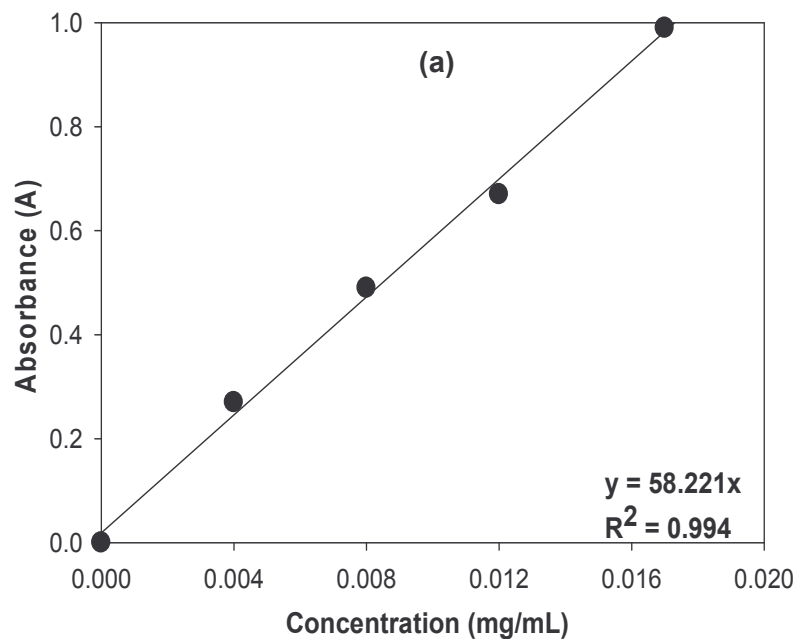


**Figure 3.1:** Calibration curves of CBZ in (a) simulated saliva (pH 6.8) and (b) simulated plasma (pH 7.4) at 285nm (N=3 and Standard Deviation  $\leq 0.029$  in all cases).

### 3.2.6.1. Model-dependent approach

This approach employed the mathematical polynomial equation. The intrinsic values of fraction of drug released over time was fitted into a second-order polynomial equation (Equation 3.1) from which the drug release rate constant ( $K_F$  in fraction/minute) were computed as the summative gradient for each profile (Equation 3.2). This parameter provided concise information

about the rate of drug release of the respective formulation under study and was useful for comparison of the profiles. All fitted curves were validated with the correlation coefficient,  $R^2$ . The statistical software (Sigma Plot, Version 11, Systat Software Inc. California, USA) was employed.

$$f(x) = a_0 + a_1 x + a_2 x^2 \quad \text{(Equation 3.1)}$$

Where  $x$  = time in minutes,  $a_0 = y$  = fractional release,  $a_1$  = slope or gradient ( $K_F$ ) and  $a_2$  = linear graphical intercept.

$$K_F = \Sigma \text{ Gradient} = \Sigma \frac{\Delta \text{ fractional drug release}}{\Delta \text{ time}} \quad \text{(Equation 3.2)}$$

Where  $K_F$  in fraction/minute is the drug release rate constant.

### 3.2.6.2. Model-independent technique

This technique used fit factors or similarity indices which comprise of the difference ( $f_1$ ) and similarity factors ( $f_2$ ) (Moore and Flanner, 1996; Anderson *et al.*, 1998; Pillay and Fassihi, 1998; Dürig and Fassihi, 2000; Sánchez-Lafuente *et al.*, 2002; Costa *et al.*, 2003). These parameters compare and establish similarities and differences between two dissolution curves obtained from a set of experimental data through a mathematical approach (Sánchez-Lafuente *et al.*, 2002). The fit factors are defined in Equations 3.3 and 3.4. The relative difference between two dissolution profiles at each experimental time is described by  $f_1$ . It approximates the percent error between two curves. The  $f_1$  value is zero when the test and reference profiles are identical and increases proportionally with the dissimilarity between the two profiles (Anderson *et al.*, 1998, Pillay and Fassihi, 1998). When two profiles are equal, this factor acquires a value from 0 to 15 while  $f_1$  value greater than 15 indicates that the two profiles are different (Sánchez-Lafuente *et al.*, 2002; Costa *et al.*, 2003). The  $f_2$  value between 50 and 100 suggests that the dissolution profiles are similar while  $f_2$  values less than 50 imply that the profiles are not similar. The  $f_2$  value of 100 suggests that the test and reference profiles are identical and as the value becomes smaller, the dissimilarity between release profiles increases (Pillay and Fassihi, 1998; Dürig and Fassihi, 2000). Each drug release profile of the model drugs under study was employed as test and reference samples for the other. The dissolution time point will be set at 8

hours (480 minutes) for both test and reference formulations throughout this investigational phase.

$$f_1 = \left\{ \frac{\sum_{t=1}^n |R_t - T_t|}{\sum_{t=1}^n R_t} \right\} \times 100\% \quad \text{(Equation 3.3)}$$

$$f_2 = 50 \log \left\{ \left[ 1 + \frac{1}{n} \sum_{t=1}^n w_t (R_t - T_t)^2 \right]^{-0.5} \times 100 \right\} \quad \text{(Equation 3.4)}$$

Where  $R_t$  is the reference assay at time point  $t$ ,  $T_t$  is the test assay at time point  $t$ ,  $n$  is the number of pull points (or time points),  $w_t$  is an optional weight factor.

### 3.2.7. Analysis of *ex vivo* permeation data

This set of data were evaluated and compared by calculating the values for drug flux ( $J_s$ ) and permeability coefficient ( $\kappa_p$ ) already described in Chapter two by Equations 2.2 and 2.3 (Section 2.2.6.2).

### 3.2.8. Comparison of the dissolution patterns of the PS and CBZ from the optimized P-RPM formulation with their commercially available counterparts

#### 3.2.8.1. Evaluation of drug release behaviour

In this section, the release patterns of PS and CBZ from the newly fabricated optimized P-RPM (containing 50mg of either PS or CBZ) intended for transbuccal drug delivery was compared with leading commercially available products namely Epanutin<sup>®</sup> (contains 100mg PS) and Tegretol<sup>®</sup>CR (contains 200mg CBZ) tablets which are administered via the oral route of drug delivery to assess its efficiency in terms of providing therapeutic effects. These products were selected for this assessment because there are no commercially available transbuccal formulation of PS and CBZ. In Chapter four, the *in vivo* performance of these set of formulation

will be evaluated and compared as well. The process described in Section 2.2.4 of Chapter two was employed to assess the drug release characteristics of these set of formulations in part. Furthermore, *in vitro* drug release from only the conventional oral tablets (Epanutin<sup>®</sup> and Tegretol<sup>®</sup>CR) were also further assessed by mimicking the gastrointestinal condition which is their original route of drug delivery. Therefore, each formulation was placed in a calibrated six-station dissolution testing apparatus (Caleva Dissolution Apparatus, model 7ST) using the standard USP 26 rotating paddle method at 50 rpm with 900mL of both pH 6.8 (small intestine) and pH 1.2 (stomach) buffer media at 37±0.5°C. All analyses were conducted in triplicate. The dissolution apparatus was modified by including a stainless steel ring mesh contrivance to prevent the hydrated formulations from floating. For the determination of PS or CBZ concentration, 5mL samples were manually withdrawn and filtered through a 0.45µm pore size Cameo Acetate membrane filter (Milipore Co., Bedford, Mass) at specific time intervals (30, 60, 120, 240, 360, and 480 minutes) over a period of 8 hours. An equivalent volume which is same as the amount withdrawn of drug-free of either buffer solution employed was replaced into the dissolution medium to maintain sink conditions. A correction factor was appropriately applied in all cases where dilutions of samples were required. The concentration of PS and CBZ released per unit time were determined spectrophotometrically at  $\lambda_{\max} = 206\text{nm}$  and  $\lambda_{\max} = 285\text{nm}$  respectively. The fit factors ( $f_1$  and  $f_2$ ) already discussed in section 3.2.6.2 of this Chapter were employed to ensure a concise comparison of generated data.

### **3.2.8.2. Preparation of calibration curves of PS and CBZ in the pH 6.8 and 1.2 phosphate buffered media**

The calibration curves for PS and CBZ in simulated saliva (pH 6.8) and plasma (pH 7.4) are already presented in Chapter two (Figure 2.3 (a) and (b); Section 2.2.12) and in this Chapter (Figure 3.1 (a) and (b); Section 3.2.5). The procedure of preparation of the calibration curves of PS and CBZ in the pH 6.8 (small intestine) and pH 1.2 (stomach) buffer media is presented in this section. The stock solution for both PS and CBZ were prepared by separately dissolving 10mg of each drug in 100mL of the buffered media solution of pH 6.8 and pH 1.2 respectively. From the stock solution, a series of dilute standard solutions of the following concentrations: 0.01, 0.03, 0.04, and 0.06 mg/mL were prepared for PS while for CBZ the following concentrations: 0.004, 0.008, 0.012 and 0.017 mg/mL were prepared by separately using the buffered media solution of pH 6.8 and pH 1.2 respectively. The absorbance of each standard solution was determined at the maximum wavelength of 206nm for PS and 285nm for CBZ and fitted into linear polynomial equations. Consequently, linear calibration curves for both PS

and CBZ in buffered media solution of pH 6.8 and pH 1.2 were respectively developed (PS: pH 6.8 buffer media;  $y=17.085x$ ;  $R^2=0.991$  and pH 1.2 buffer media;  $y=16.694x$ ;  $R^2=0.995$  while for CBZ: pH 6.8 buffer media;  $y=58.004x$ ;  $R^2=0.989$  and pH 1.2 buffer media;  $y=59.092x$ ;  $R^2=0.999$ ) were constructed respectively (Figures 3.2 (a) - (d)).

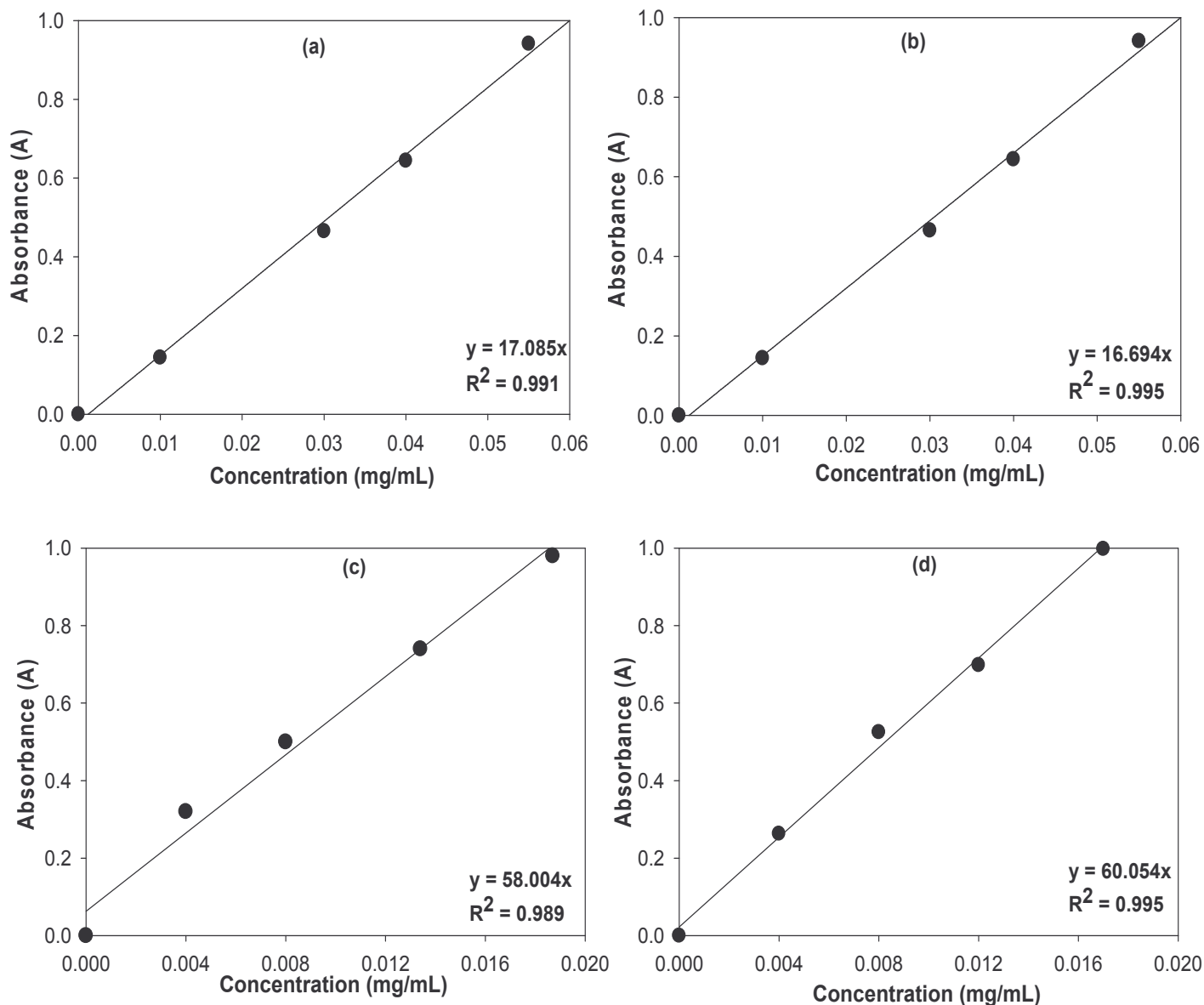


**Figure 3.2:** Calibration curves of: (a) PS in pH 6.8 buffer media, (b) PS in pH 1.2 buffer media at 206nm and (c) CBZ in pH 6.8 buffer media, (d) CBZ in pH 1.2 buffer media at 285nm (N=3 and Standard Deviation  $\leq 0.051$  in all cases).

### 3.3. RESULTS AND DISCUSSION

#### 3.3.1. Systematic characterization and comparison of the physicochemical properties of the PS and CBZ loaded optimized P-RPM formulations

##### 3.3.1.1. Physical appearance and weight

Typically, both PS and CBZ P-RPM formulations were similar as regards their physical appearance. They were whitish, compact with a convex-shaped base and flat surface on the other side. Each had an average diameter of  $8 \pm 1$ mm and thickness of  $4 \pm 0.5$ mm. A photograph of the PS and CBZ loaded matrices is shown in Figure 3.3. Each matrix had an average weight of  $171.28 \pm 4.69$  mg.

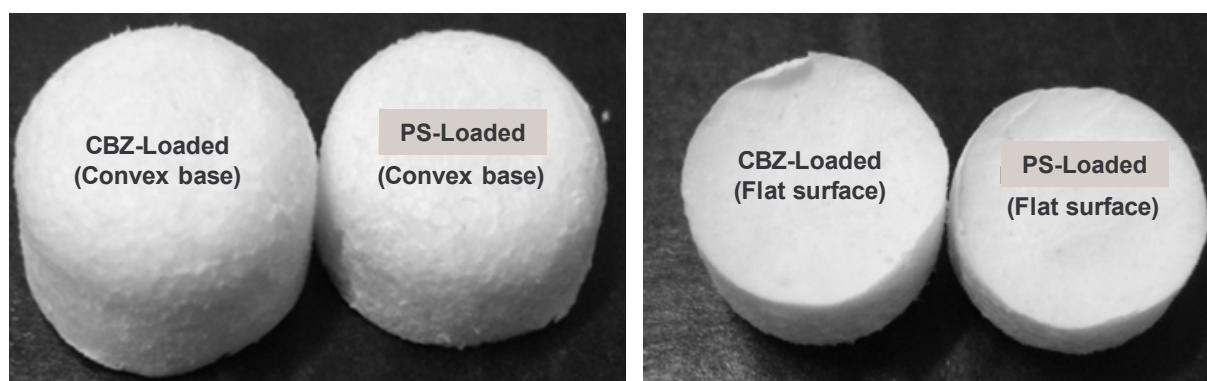


**Figure 3.3:** Digital photographs showing the similarity in physical appearance of the optimized PS and CBZ loaded P-RPM formulations.

##### 3.3.1.2. Drug loading capacity, *ex vivo* bioadhesivity, quantitative matrix porosity and rheological parameters

Table 3.1 presents the values obtained for the drug loading capacity, bioadhesive strength, quantitative measure of matrix porosity and blend rheology measured as deformation and viscosity for both PS and CBZ loaded P-RPM formulations.

**Table 3.1:** Some physicochemical measures highlighting possible similarities and differences between the PS and CBZ loaded formulation matrices

Measured Parameters	PS <sup>a</sup> - loaded Formulation	CBZ <sup>b</sup> - loaded Formulation
Work of adhesion (J)	0.0039 ± 0.0002	0.0034 ± 0.0006
Bioadhesive force (N)	1.1810 ± 0.0500	1.0751 ± 0.0210
Drug loading capacity (%)	99.7200 ± 3.5600	90.0541 ± 1.1500
Pore width (Å)	86.0116 ± 4.0405	80.1233 ± 3.4200
Viscosity (mPa.s)	1.0400×10 <sup>4</sup> ± 0.002×10 <sup>4</sup>	2.0510×10 <sup>4</sup> ± 0.002×10 <sup>4</sup>
Rheological deformation	1.5161×10 <sup>4</sup>	1.5074×10 <sup>4</sup>

<sup>a</sup> Phenytoin sodium, <sup>b</sup> Carbamazepine

Slight differences were observed in the values of the physicochemical measures obtained as outlined in Table 3.1. Overall, this may be attributable to the possible impact of CBZ on the matrix integrity before and after lyophilization due to its low aqueous solubility. With respect to measures for bioadhesive strength, the CBZ formulations displayed lower levels (0.0034J and 1.0751N) than that of PS formulations (0.0039J and 1.1810N) which may be due to the effect of CBZ solubility on the interactive forces initiating and sustaining mucoadhesion between formulation and the buccal mucosa. The CBZ formulation had lower drug loading capacity values (90.0541%) than the PS formulation (99.7230%) and may be as a result of the influence of CBZ on the level of dispersion of drug molecules within the homogenous blend.

Both PS and CBZ optimized formulations remained mesoporous in nature as the experimental design formulations explored in Chapter two. However, the average width/sizes of the pores formed within the CBZ formulation matrix were smaller (80.1233 Å) than those of the PS formulations (86.0116 Å). This can be related to the higher viscosity values displayed by the CBZ homogenous blend (2.0510×10<sup>4</sup> mPa.s) indicating its capability to enhance the intrinsic stiffness within the homogenous blend milieu. This may directly slow down velocity of mobile liquid molecules during the processes of pre-freezing and sublimation during lyophilization thereby generating smaller, tighter intra-matrix pore sizes.

Furthermore, the rheological deformation values of the PS (1.5161×10<sup>4</sup>) and CBZ (1.5074×10<sup>4</sup>) were closely related and this may imply that despite the differences in the physical properties of CBZ, its introduction into the optimized co-particulate homogenous blend did not distort its stable internal configuration or influence its chemical structural network or backbone. In other

words, the physical properties of the component compounds of the homogenous blends were retained despite the introduction of CBZ.

### 3.3.1.3. Examination of the surface porous structure

Both the PS and CBZ loaded P-RPM formulations displayed a unique porous surface structure. Scanning electron micrographs showing the surface geometry of the two are presented in Figure 3.4 (a) and (b). Both matrices showed irregular pore and interconnector structures occupying a wide surface area. The PS formulation has multifaceted pores with varying widths and relatively solid, uneven interconnectors. Its porous geometry resembles a mono-layered sheet (Figure 3.4 (a)).

The CBZ matrix on the other hand can be described as having knitted, spongy pore structures and spiked interconnectors (Figure 3.4 (b)). Its porous structure can be said to be multi-layered and more widely distributed as opposed to the PS loaded formulation. The differences between the PS and CBZ formulations may be attributable to the differences in their solubilities. The nature of layers within the porous network of the formulations may influence the process of penetration of water molecules.

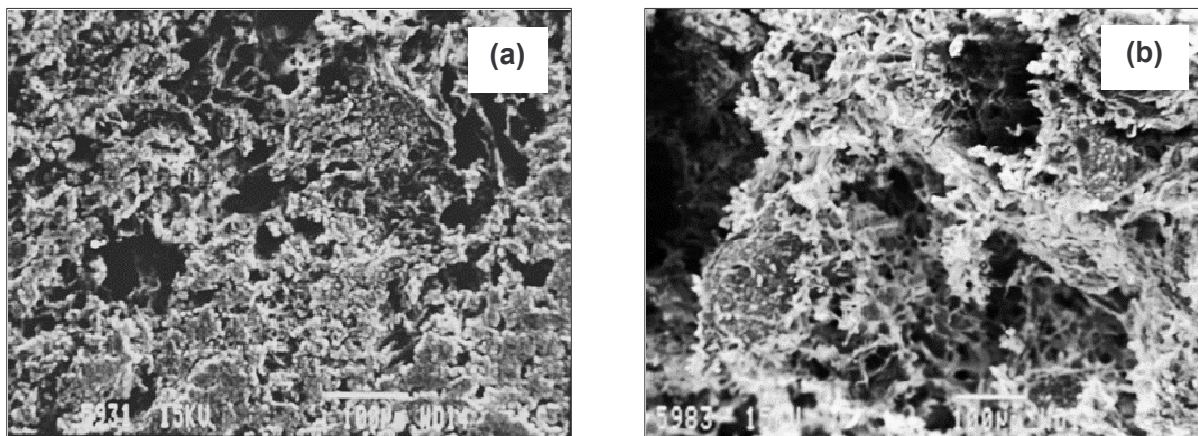


**Figure 3.4:** Scanning electron micrographs of the (a) PS and (b) CBZ optimized P-RPM formulations showing the characteristic pore structures, distributions and interconnectors (magnification 1000 $\times$ ).

### 3.3.1.4. *In vitro* drug release behaviour

#### 3.3.1.4.1. Comparison of drug release performance of the PS and CBZ loaded P-RPM formulations

The drug release performances of the PS and CBZ loaded formulations based on the generated profiles were relatively different in appearance (Figure 3.5). The CBZ loaded formulation demonstrated a slower release rate (90.74% in 8 hours) than the PS loaded matrix (97.54% in 8 hours) attributable to the lower solubility of CBZ compared with PS (Figure 3.5). It can be proposed that CBZ enhanced matrix stiffness and hydrophobicity which may reduce the rate at which the processes of matrix wetting, loosening and dissolution occur thereby influencing the rate of drug dissolution and liberation. This proposition was further substantiated by the outcome of the scanning electron microscopic examinations (Figure 3.4) in which case the CBZ matrix appeared as a multi-layered closely knitted platform as opposed to the mono-layered PS matrix. In other words, the more rigid porous network of the CBZ loaded matrix may serve as a stronger barrier to the penetration of water molecules to initiate the process of matrix immobilization which determines the rate of drug release as opposed to the PS loaded matrix.

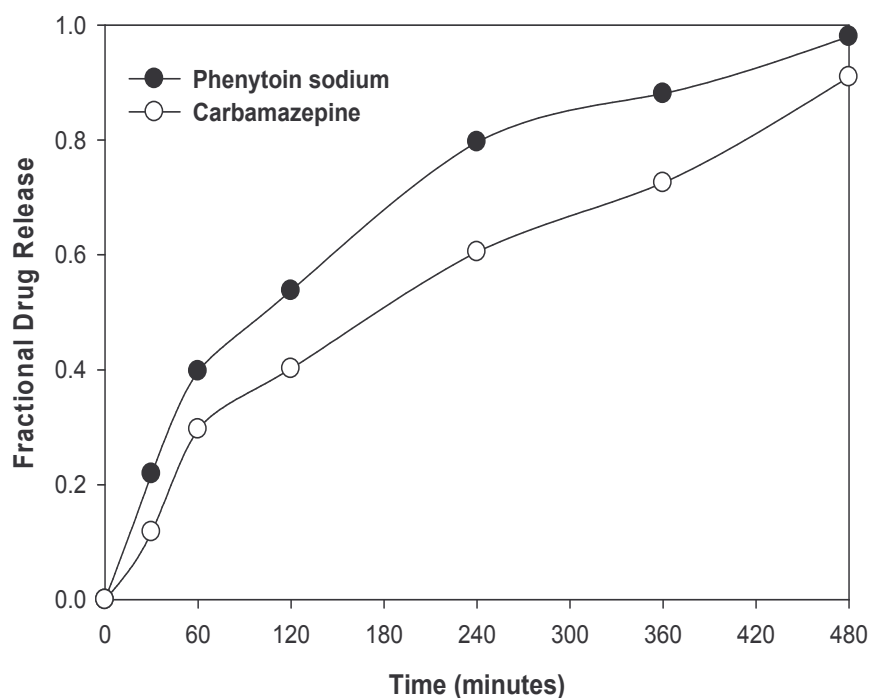


**Figure 3.5:** Fractional release profiles for PS and CBZ in simulated saliva, pH 6.8 over 8 hours (N = 3 and Standard Deviation  $\leq 0.055$  in all cases).

Furthermore, the release profiles shown in Figure 3.5 above was evaluated by computing concise numerical values for the drug release rate constant ( $K_F$ ) and the difference ( $f_1$ ) and similarity ( $f_2$ ) factors (Table 3.2).

**Table 3.2:** Parameters utilized to capture and compare the drug release performances of the PS and CBZ loaded matrix formulations

Formulations	$K_F^c$ (fraction/minute)	$R^2^d$	$f_1^e$	$f_2^f$
PS <sup>a</sup>	0.004	0.949	7.191	60.016
CBZ <sup>b</sup>	0.003	0.966	7.750	55.916

<sup>a</sup> Phenytoin sodium, <sup>b</sup> Carbamazepine, <sup>c</sup> Drug release rate constant, <sup>d</sup> Correlation coefficient, <sup>e</sup> Difference factor, <sup>f</sup> Similarity factor

The values of  $K_F$  for both formulations were slightly different with the CBZ loaded formulation having a lower value (0.003fraction/minute) than the PS loaded formulation (0.004fraction/minute). This implied that the inclusion of CBZ into the P-RPM matrix formulation slowed down the rate/speed/velocity at which drug molecules are released relative to drug release from the PS loaded formulation. This behaviour can be attributed to the low solubility of CBZ as compared to PS.

However, the similarity and difference factors ( $f_1$  and  $f_2$ ) revealed that overall, the two profiles can be said to be similar or comparable at each experimental time as  $f_1$  gave values in-between 0 and 15 and  $f_2$  was between 50 and 100. Therefore, it can be hypothesized that the pore-regulated polymer matrix developed in this study is a robust, adaptable drug delivery system that may be applied for controlled delivery of both high and low solubility drugs without significantly influencing the matrix stability. In other words, drug release from this novel matrix may not be solely dependent on drug solubility levels but also well regulated by polymeric matrix characteristics.

### 3.3.1.5. *Ex vivo* drug permeation

The PS and CBZ loaded P-RPM formulations showed the capability to consistently initiate and sustain the permeation of both drug molecules from the donor compartment (simulated saliva medium) through the model buccal mucosal tissue into the receiving compartment of the Franz diffusion cells (simulated plasma medium) over the period of 8 hours. A close to linear, sustained permeation of the drug molecular species was observed over time. This suggests passive diffusion initiated and maintained by the drug loaded P-RPM formulations to be the

possible mechanism of drug permeation (Figure 3.6). Also, the consistent increment in the percentage of drug molecules which permeated over time may indicate that the mucosal sites for permeation were not saturated with either of the model drugs over the period of exposure to the optimized P-RPM formulations. Representative *ex vivo* drug permeation profiles of the optimized P-RPM formulation loaded with either PS or CBZ are shown in Figure 3.6.

Both PS and CBZ permeation patterns may be described as bi-phasic because a sharp, linear increase in drug permeation levels up to the 4<sup>th</sup> hour (240 minutes) followed by slight increments resembling a plateau up to the 8<sup>th</sup> hour (480 minutes) (Figure 3.6). This observed trend may be of an advantage as the initial rapid linear increase in drug permeation levels can initiate pharmacotherapeutic actions and relief to the patient while the second phase maintains the plasma levels of drug molecules thereby enhancing reduction of dosage frequencies and possibly enhancing patient compliance. In addition, the PS formulation displayed a slightly faster permeation velocity than the CBZ formulation. This may be associated with the distinct differences in the aqueous solubilities of the two model drugs (PS: 100mg/mL at 25°C; CBZ: 0.01mg/mL at 25°C). Also, it can be inferred that the effect of the differences in the aqueous solubility levels of PS and CBZ impacted their permeation capabilities at the buccal mucosal sites more than the differences in their permeability coefficient values (PS:  $\log P = 2.14$ ; CBZ:  $\log P = 2.93$ ) as PS possessing a higher aqueous solubility and lower permeability potential permeated through the mucosal sites at a slightly higher level than its counterpart, CBZ (Figure 3.6).

Also, the differences between the PS and CPZ formulations were visualized by evaluating the changes in drug flux (quantity of drug that permeates per cross-sectional area per minute or over time). Both PS and CBZ formulations displayed a similar trend the changes in flux values over time typified by an initial increase at 30 minutes followed by gradual decrease over time (Figure 3.7). The flux values measured per unit time were higher for the PS loaded formulation. This may still be associated with the differences in solubilities of PS and CBZ. Consequently, an explanation that the PS molecules possess a greater potential to dissolve in the water-based medium (simulated plasma and saliva) thereby aiding the process of diffusion through the model buccal mucosal membrane can be put forward. The CBZ molecules on the other hand are less miscible with the water-based microenvironment resulting in a reduced permeation potential.

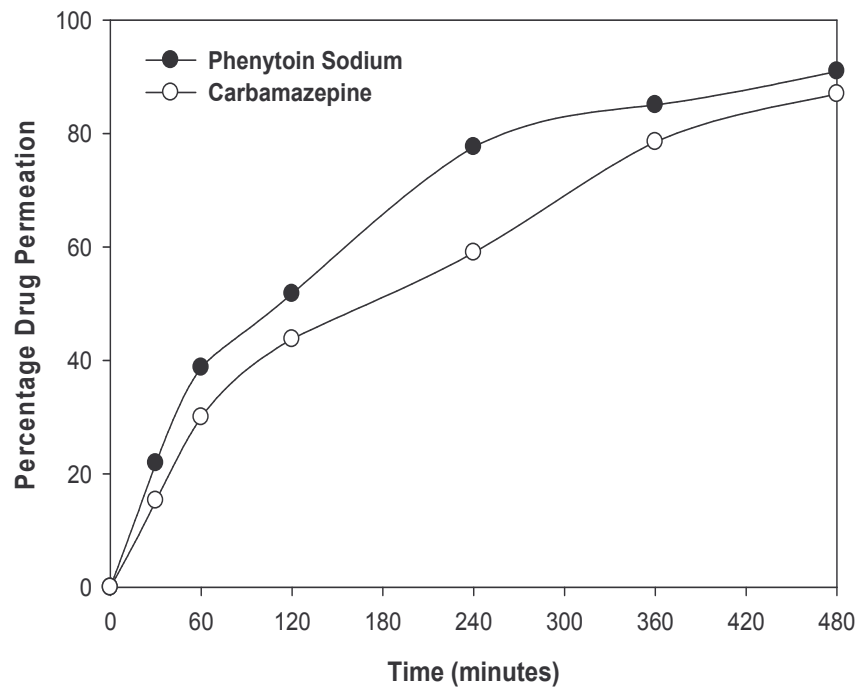


**Figure 3.6:** Permeation of PS and CBZ molecules into simulated plasma, pH 7.4 through the porcine buccal mucosa over 8 hours (N = 3 and Standard Deviation  $\leq 5.77\%$  in all cases).

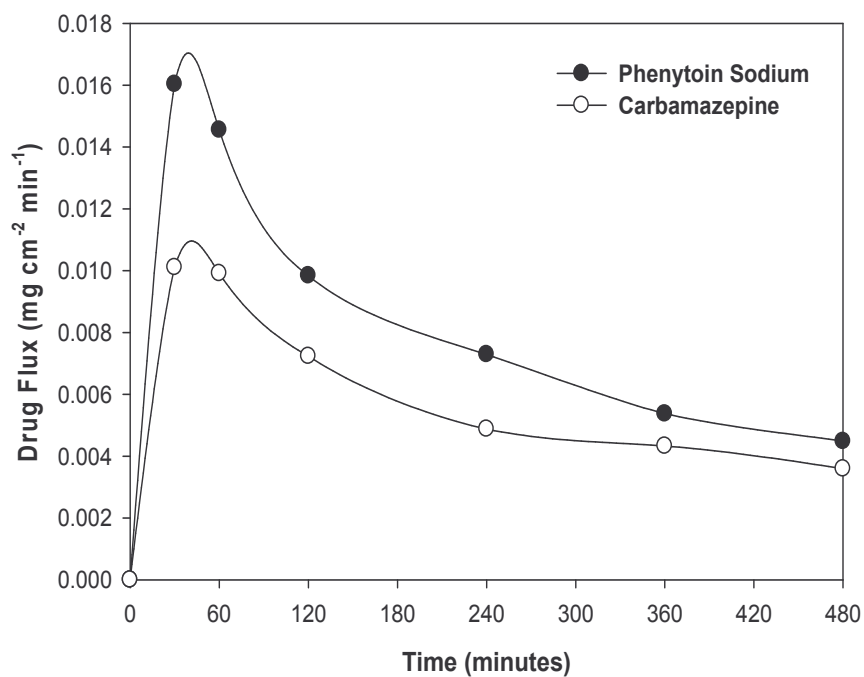


**Figure 3.7:** Changes in steady state flux with time over 8 hours (N = 3 and Standard Deviation  $\leq 2.01 \times 10^{-4} \text{ mg cm}^{-2} \text{ min}^{-1}$  in all cases).

Changes in permeability coefficient over time for both formulations were observed (Figure 3.8). Overall, an increase was observed with time. The PS formulation had higher permeability coefficient values than the CBZ formulation. Based on the mathematical expression representing permeability coefficient (Equation 2.3), it can be described as the velocity of drug diffusion, that is, the change in distance per unit time. With both PS formulations, a progressive increase in the distance traveled by the drug molecules was noted over time but the permeability coefficient values obtained was higher for PS than CBZ due to the differences in their solubilities. Therefore, the PS possesses a slightly greater momentum to permeate the buccal tissue than CBZ when in solution in the water-based media.

On the whole, it can be proposed that the optimized P-RPM possesses the potential to initiate and sustain the *ex vivo* permeation of drug molecules of both high or low solubility and high or low permeability potentials as the profiles generated for PS and CBZ were quite comparable in their trends.

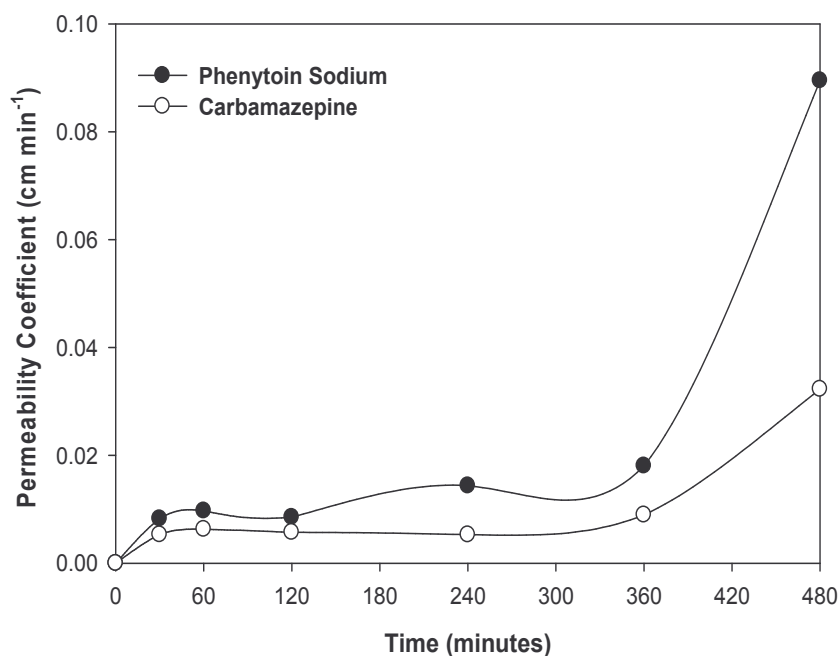


**Figure 3.8:** Changes in permeability coefficient with time over 8 hours (N = 3 and Standard Deviation  $\leq 3.99 \times 10^{-3} \text{ mg cm}^{-2} \text{ min}^{-1}$  in all cases).

### 3.3.2. Assessment of physicochemical properties by textural analysis

The measures of physicochemical strength quantified for both formulations include the matrix resilience ( $M_R$ ), energy of matrix distortion ( $\epsilon_D$ ) and matrix firmness ( $M_F$ ) and are outlined in Table 3.3.

**Table 3.3:** Parameters utilized to capture and compare the drug release performances of the PS and CBZ loaded matrix formulations

Formulations	$M_R^c$ (%)	$\epsilon_D^d$ (J)	$M_F^e$ (N/mm)
PS <sup>a</sup>	2.897	0.048	4.192
CBZ <sup>b</sup>	5.504	0.029	8.549

<sup>a</sup> Phenytoin sodium, <sup>b</sup> Carbamazepine, <sup>c</sup> Matrix resilience, <sup>d</sup> Matrix distortion, <sup>e</sup> Matrix firmness

A difference in the numerical values of the measured physicochemical parameters was notable for the PS and CBZ formulations. The CBZ formulations displayed relatively higher values as regards matrix resilience and firmness with a lower magnitude for the energy of matrix distortion while the converse is true for the PS formulation. Therefore, the CBZ formulation can be described as being reasonably mechanically stronger than the PS formulation. This may be attributable to the hydrophobic tendencies of CBZ relative to PS as well as CBZ or PS interactions with the polymer matrix. With matrix resilience, the CBZ loaded matrix displayed a better capability to recover from the effect of an applied external compressive strain indicating that the CBZ matrix is more elastically cohesive than the PS formulation. In addition, the CBZ formulation appears to be more resistant to permanent deformation from an external force and higher energy levels required to be absorbed to overcome the intrinsic matrix forces as lower energy levels are dissipated to the environment compared to the PS formulation (a measure of matrix firmness and energy of deformation) (Table 3.2). This outcome may be related to the differences in their surface morphologies as the CBZ formulation appeared as a tighter, multi-layered matrix while the PS formulation was mono-layered with a loose internal network (Figure 3.4). Overall, the differences in the physicochemical strength of the CBZ and PS P-RPMs play a significant role in influencing their exhibited physicochemical behaviour.

### 3.3.3. Comparing the *in vitro* release characteristics of the PS or CBZ loaded P-RPM formulations with the commercially available products

For both the PS and CBZ loaded formulations, the newly designed optimized P-RPM formulation demonstrated a more controlled and consistent drug release characteristics with

minimal initial burst effect at the first hour as compared to the conventional products (Epanutin<sup>®</sup> and Tegretol<sup>®</sup>CR) which exhibited much higher burst release effects coupled with rapid and irregular trends of drug release (Figures 3.9 and 3.10).

Additionally, the levels of similarity/dissimilarity amongst the generated release profiles in Figures 3.9 and 3.10 below were further evaluated by computing the difference ( $f_1$ ) and similarity ( $f_2$ ) factors (Tables 3.4 and 3.5 ) employing each profile as a reference for the other. The outcome of this analytical approach further substantiates the observed differences in the dissolution trends of the P-RPM formulations and the commercial products (Table 3.4). Besides, the values of  $f_1$  and  $f_2$  obtained from the comparison of the drug release profiles generated by Epanutin<sup>®</sup> and Tegretol<sup>®</sup>CR subjected to different dissolution conditions shows similarity in their trends (Table 3.5).

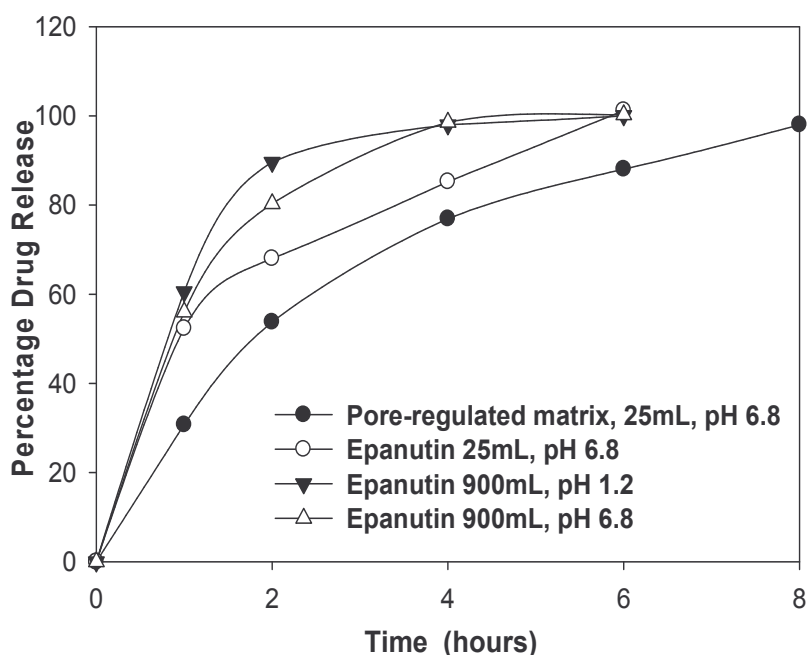


**Figure 3.9:** Drug release profiles of the optimized P-RPM formulation loaded with PS in simulated saliva (pH 6.8) compared with those of Epanutin<sup>®</sup> in 25mL simulated saliva (pH 6.8), 900mL simulated gastric fluid (pH 1.2) and simulated intestinal fluid (pH 6.8) (N = 3 and Standard Deviation ≤ 5.67% in all cases).

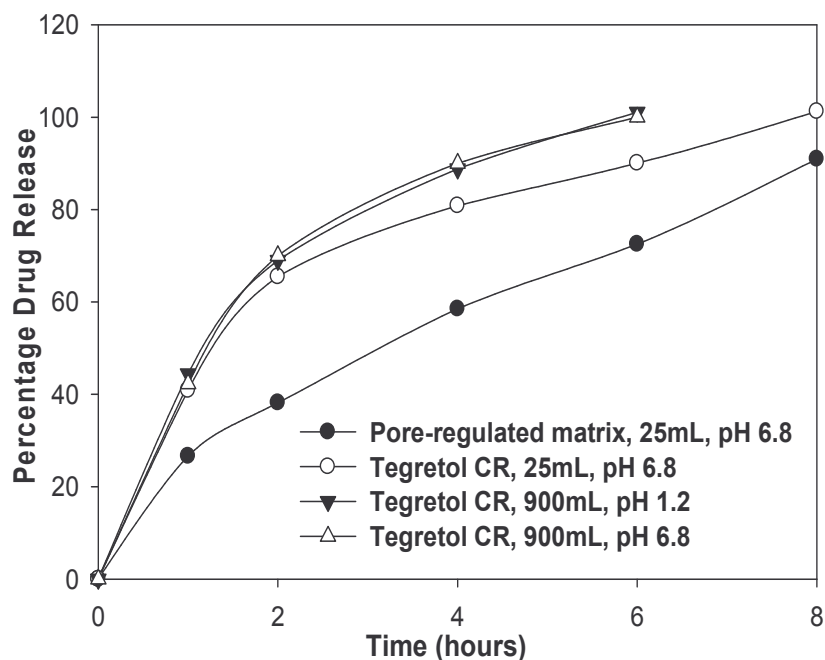


**Figure 3.10:** Drug release profiles of the optimized P-RPM formulation loaded with CBZ in simulated saliva (pH 6.8) compared with those of Tegretol<sup>®</sup>CR 25mL in 25mL simulated saliva (pH 6.8), 900mL simulated gastric fluid (pH 1.2) and simulated intestinal fluid (pH 6.8) (N = 3 and Standard Deviation ≤ 7.02% in all cases).

**Table 3.4:** Computed difference and similarity factors to compare the drug release performances of the P-RPM formulations with the commercially available products

Formulations	$f_1^e$	$f_2^f$
PS-P-RPM <sup>a</sup>	29.785	6.052
CBZ-P-RPM <sup>b</sup>	36.535	11.552
Epanutin <sup>®</sup> -1 <sup>c</sup>	19.998	9.812
Tegretol <sup>®</sup> CR-1 <sup>d</sup>	21.796	14.447

<sup>a</sup> P-RPM loaded with phenytoin sodium, <sup>b</sup> P-RPM loaded with carbamazepine, <sup>c</sup> Epanutin<sup>®</sup> in 25mL simulated saliva (pH6.8), <sup>d</sup> Tegretol<sup>®</sup>CR in 25mL simulated saliva (pH6.8), <sup>e</sup> Difference factor, <sup>f</sup> Similarity factor

**Table 3.5:** Employing the difference and similarity factors to compare the drug release behaviour of the commercially available products subjected to different dissolution conditions

Formulations	$f_1^g$	$f_2^h$
Epanutin <sup>®</sup> -1 <sup>a</sup>	2.365	66.912
Epanutin <sup>®</sup> -2 <sup>b</sup>	7.566	54.994
Epanutin <sup>®</sup> -3 <sup>c</sup>	5.605	78.952
Tegretol <sup>®</sup> CR-1 <sup>d</sup>	10.201	80.002
Tegretol <sup>®</sup> CR-2 <sup>e</sup>	9.956	65.255
Tegretol <sup>®</sup> CR-3 <sup>f</sup>	8.723	71.118

<sup>a</sup> Epanutin<sup>®</sup> in 25mL simulated saliva (pH6.8), <sup>b</sup> Epanutin<sup>®</sup> in 900mL buffer media (pH1.2), <sup>c</sup> Epanutin<sup>®</sup> in 900mL buffer media (pH6.8), <sup>d</sup> Tegretol<sup>®</sup>CR in 25mL simulated saliva (pH6.8), <sup>e</sup> Tegretol<sup>®</sup>CR in 900mL buffer media (pH1.2), <sup>f</sup> Tegretol<sup>®</sup>CR in 900mL buffer media (pH6.8), <sup>g</sup> Difference factor, <sup>h</sup> Similarity factor

### 3.4. CONCLUDING REMARKS

In this chapter, the optimized P-RPM formulation have been successfully explored and characterized based on its physicochemical and physicomachanical properties. The influence of the differences in drug solubility and permeability levels on the performance of the newly developed P-RPM formulation was also investigated by utilizing PS and CBZ. The optimized P-RPM formulation has proved to be a stable and robust matrix for transbuccal drug delivery as the inclusion of either PS or CBZ with different physicochemical properties did not drastically alter its physicochemical and physicomachanical performances. Certainly, some disparities attributable to the differences in the physicochemical properties of both model drug species were observed. Furthermore, the comparison of the *in vitro* drug release performance of the P-RPM formulation with those of the commercially available oral tablet products showed that the P-RPM possessed the capability to control and sustain drug release as opposed to the conventional formulations. On the whole, the P-RPM formulation developed in this study may be described as a versatile, controlled release drug delivery system which may possibly be applied to wide variety drugs with differing solubility and permeability levels. The next chapter will be exploring the *in vivo* performance of the optimized P-RPM formulation by quantitatively and qualitatively determining the plasma drug levels. Also, pharmacokinetic and pharmacodynamic modeling of the generated plasma concentration profiles will be performed. Both PS and CBZ loaded formulations will be utilized for this phase of the investigation.